

Techniques to reduce memory needs for coupled photon-electron transport.

Bruno Turcksin, Jean Ragusa, and Jim Morel

Texas A&M University, Department of Nuclear Engineering

College Station, Texas 77843-3133

turcksin@neo.tamu.edu; ragusa@ne.tamu.edu; morel@ne.tamu.edu

ABSTRACT

In this work, we present two methods to decrease memory needs while solving the photon-electron transport equation. The coupled transport of electrons and photons is of importance in radiotherapy because it describes the interactions of X-rays with matter. One of the issues of discretized electron transport is that the electron scattering is very forward peaked. A common approximation is to represent the peak in the scattering cross section by a Dirac distribution. This is convenient, but the integration over all angles of this distribution requires the use of Galerkin quadratures. By construction these quadratures impose that the number of flux moments be equal to the number of directions (number of angular fluxes), which is very demanding in terms of memory. In this study, we show that even if the number of moments is not as large as the number of directions, an accurate solution can be obtained when using Galerkin quadratures. Another method to decrease the memory needs involves choosing an appropriate reordering of the energy groups. We show in this paper that an appropriate alternation of photons/electrons groups allows us to rewrite one transport problem of n groups as gcd successive transport problems of $\frac{n}{gcd}$ groups where gcd is the greatest common divisor between the number of photon groups and the number of electron groups.

Key Words: Galerkin quadrature, photon-electron transport, radiotherapy

1. Introduction

The transport of photons and electrons has many applications in medical physics and particularly in radiotherapy. Radiotherapy uses photons and charged particles to damage the DNA of cancerous cells. While using photons, free electrons are created; this ionizes the environment and creates free radicals that damage the cells DNA. One quantity used to gauge whether a cell will die due to radiation is the absorbed dose, defined as the energy deposited per unit of mass and measured in Gray ($Gy = \frac{J}{kg}$). Several methods can be applied to solve the photon-electron distribution in the body : semi-analytic methods, deterministic methods and Monte-Carlo methods. Monte-Carlo methods yield very accurate results, however they are slow to converge and thus, remain too slow for effective clinical use [1]. Other methods, such as pencil-beam convolution and convolution-superposition, employ pre-calculated Monte-Carlo dose kernels, which are then locally scaled to approximate photon and electron transport in the presence of heterogeneities. These methods present some issues in the presence of large density gradients, such as those found at interfaces between different materials: air, bone, lung and soft tissue [1–3]. If enough cells are used, deterministic methods can be accurate even on interfaces between materials [1]. These methods are faster than Monte-Carlo methods but slower than the semi-analytic

methods.

In this work, we present a S_n method for photon-electron transport. The difficulty of this calculation comes from the transport of the electrons. Because the electrons are charged particles, they have very anisotropic scattering due to their interactions with other particles through Coulomb interaction. This anisotropy causes some complications since the standard Legendre expansion representing the cross sections would require hundreds of terms. A common approximation is to use a Dirac distribution to model the forward-peaked scattering of the electrons and a continuous slowing down term for energy loss due to Coulomb interactions. This allows the Legendre expansion of the cross section to be kept to a low order. However, an exact integration of the Dirac distribution requires to use Galerkin quadratures [4] that demand a significant amount of memory. These quadratures need the number of flux moments and the number of angular fluxes to be equal and this number varies as $\frac{n(n+2)}{8}$ per octant with the order of the S_n method. For example, when using the S_n discretization for $n = 16$, we have, in 3D, 288 directions and thus, 288 angular fluxes or flux moments to store.

In this work, we analyze the effects of truncation on the Galerkin quadratures. To do this, we alter the order of the scattering cross sections and observe the effect on the absorbed dose. The goal is to keep as few flux moments as possible while maintaining an accurate solution. We also show a method of ordering the energy groups which allows to decompose one large transport problem in several smaller transport problems. This interesting possibility is due to the fact that there is no thermalization of the particles. Therefore, every particle undergoes only slowing down and the scattering matrix can be written as a lower block triangular matrix. The interactions between photons and electrons forbids a lower triangular matrix by adding some upscattering terms in the scattering matrix. The code generating the cross sections, CEPXS [5], generates first the cross sections for one particle type and then, the cross sections for the other one. We show in this paper how to improve the order of the groups.

2. Equations

In this section, we present the equation that models the transport of electrons. We will also show why it is so important to use Galerkin quadratures. First, we present the Boltzmann-Fokker-Planck equation (BFP). The idea is to decompose the highly forward peaked scattering cross section into a sum of a forward-peaked cross section and a smoothly varying cross section. The BFP equation is given by (the variables are omitted for brevity) [6] :

$$\begin{aligned} \boldsymbol{\Omega} \cdot \boldsymbol{\nabla} \Psi + \Sigma_t \Psi = & \int_{4\pi} \int_0^\infty \Sigma_s (\boldsymbol{\Omega} \cdot \boldsymbol{\Omega}', E' \rightarrow E) \Psi(\boldsymbol{\Omega}', E') dE' d\boldsymbol{\Omega}' \\ & + \frac{\alpha}{2} \left(\frac{\partial}{\partial \mu} (1 - \mu^2) \frac{\partial \Psi}{\partial \mu} + \frac{1}{1 - \mu^2} \frac{\partial^2 \Psi}{\partial \phi^2} \right) + \frac{\partial S \Psi}{\partial E} + Q \end{aligned} \quad (1)$$

where :

- Ψ is the angular flux
- Σ_t is the smooth-component of the total macroscopic cross section
- Σ_s is the smooth-component of the macroscopic differential scattering cross section
- Q is a volumetric source

- μ is the cosine of the directional polar angle
- ϕ is the directional azimuthal angle

The second and the third term of the right-hand-side change the direction of the particles without changing their energy and the fourth term changes the energy of the particles without changing their direction (continuous slowing-down term) [7]. The continuous slowing down is used for the “soft” interactions that result in small-energy losses. The catastrophic interactions that result in large energy losses are represented with the standard Boltzmann operator. α is the restricted momentum transfer :

$$\alpha(E) = 2\pi \int_0^E \int_{-1}^1 \Sigma_{ss}(E \rightarrow E', \mu_0)(1 - \mu_0) d\mu_0 dE' \quad (2)$$

with $\mu_0 = \mu'\mu + \sqrt{(1 - \mu'^2)(1 - \mu^2)}\cos(\phi' - \phi)$ and $\Sigma_{ss}(E \rightarrow E', \mu_0)$ denotes the forward-peaked scattering cross section.

S is the restricted stopping power :

$$S(E) = 2\pi \int_0^E \int_{-1}^1 \Sigma_{ss}(E \rightarrow E', \mu_0) (E - E') d\mu_0 dE' \quad (3)$$

The restricted stopping power is defined as the portion of the total stopping power that is not due to catastrophic collisions.

Standard boundary conditions can be applied to (1), the most likely being the vacuum boundary conditions :

$$\Psi(\mathbf{r}, \boldsymbol{\Omega}, E) = 0 \quad \text{for } \boldsymbol{\Omega} \cdot \mathbf{n} < 0 \text{ and } \mathbf{r} \in \partial\mathcal{D}_v \quad (4)$$

and the incoming flux boundary conditions :

$$\Psi(\mathbf{r}, \boldsymbol{\Omega}, E) = g(\mathbf{r}, \boldsymbol{\Omega}, E) \quad \text{for } \boldsymbol{\Omega} \cdot \mathbf{n} < 0 \text{ and } \mathbf{r} \in \partial\mathcal{D}_i \quad (5)$$

where $\partial\mathcal{D}_v$ is the boundary of the domain where vacuum conditions are applied and $\partial\mathcal{D}_i$ is the boundary of the domain where incoming flux conditions are applied.

In this work, we will use another approach and retain only the asymptotic limit on the energy dependence but not the angular dependence. We will keep the continuous slowing-down term and approximate the forward peaked angular dependence by a Dirac distribution. The equation can be written as :

$$\boldsymbol{\Omega} \cdot \nabla \Psi + \Sigma_t \Psi = \int_{4\pi} \int_0^\infty \Sigma_s(\boldsymbol{\Omega} \cdot \boldsymbol{\Omega}', E' \rightarrow E) \Psi(\boldsymbol{\Omega}', E') dE' d\boldsymbol{\Omega}' + \int_{-1}^1 c\delta(\mu-1)\Psi d\mu + \frac{\partial S\Psi}{\partial E} + Q \quad (6)$$

The continuous slowing-down term in the equation (6) can be either treated explicitly or it can be treated in the cross sections. The latter was done in the CEPXS code which produces cross sections for photons and electrons transport [5]. In this work, we use cross sections produced by CEPXS to compute the coupled photon-electron transport. Unlike [1], we do not assume that the electrons do not produce photons. The system is fully coupled, meaning that photons produce electrons and electrons produce photons. Thus, there are some upscattering terms present in the scattering matrix even if there is not upscattering physically. The upscattering is between particle types; a given particle can only loses energy and creates others particle types which are represented by the upscattering terms.

Next, we focus on the scattering term, assuming that this quantity has been integrated over the energy range :

$$R = \int_{4\pi} \Sigma_s (\boldsymbol{\Omega} \cdot \boldsymbol{\Omega}') \Psi (\boldsymbol{\Omega}') d\boldsymbol{\Omega}' + \int_{-1}^1 c\delta(\mu - 1)\Psi d\mu \quad (7)$$

In a S_n code, it is usual to write the discretized scattering source (7) as a product of 3 matrices [4] :

$$\mathbf{R} = \mathbf{M}\mathbf{\Sigma}\mathbf{D}\mathbf{\Psi} \quad (8)$$

where \mathbf{R} is the vector containing the scattering source, $\mathbf{\Psi}$ is the vector containing all the flux moments, \mathbf{D} is the discrete-to-moment matrix which maps a vector of discrete angular flux values to a corresponding vector of flux moments, $\mathbf{\Sigma}$ is the scattering matrix which contains the moments of the scattering cross sections on its diagonal, and \mathbf{M} is the moment-to-discrete matrix which maps a vector of flux moments to a corresponding vector of discrete angular flux values. The Galerkin quadratures require that :

$$\mathbf{D} = \mathbf{M}^{-1} \quad (9)$$

and, therefore, \mathbf{M} and \mathbf{D} have to be square matrices. This implies that the number of moments is equal to the number of directions.

Galerkin quadratures integrate exactly a delta function scattering and that is why we need to use them. To see this, assume that :

$$\Sigma(\mu) = \delta(\mu - 1) \quad (10)$$

It is obvious that :

$$\begin{aligned} R &= \int_{-1}^1 \delta(\mu - 1)\Psi(\mu)d\mu \\ &= \Psi \end{aligned} \quad (11)$$

Because $P_l(1) = 1$ for all l , all of the Legendre expansion coefficients, Σ_l , for the delta function equal to unity and the cross-section matrix is the identity matrix. We get :

$$\mathbf{R} = \mathbf{M}\mathbf{D}\mathbf{\Psi} = \mathbf{\Psi} \quad (12)$$

3. Memory issues

In the previous section, we showed that we must use a Galerkin quadrature to solve (6) correctly. This may be a significant issue in terms of memory requirements. For neutron transport, the scattering is less anisotropic than for electron transport, and therefore, fewer flux moments than angular fluxes are needed. This is the reason why the information is stored as flux moments. However, Galerkin quadratures require the number of moments to be equal to the number of directions. This requirement is very restrictive and it is important to explore whether it is possible to decrease the number of moments while keeping a larger number of directions. In [8], the authors used a Legendre expansion of the scattering cross section lower than that required by the Galerkin quadrature. They have shown a good agreement between their results and Monte-Carlo simulations. In the next section, we will study the effects of changing the order of the Legendre expansion while keeping a larger number of angular fluxes than the order of

the scattering expansion. We proceed by building the matrices M and D using the Galerkin quadrature, then truncate them to keep only a few moments. Therefore, M and D will be rectangular instead of square matrices. We show the results for two materials (Al and Au) and for different Legendre expansions.

4. Results

In this section, we compare our results using PDT with the ones computed using ONELD[5]. PDT is a three dimensional Parallel Deterministic Transport code developed at Texas A&M University while ONELD is a code that solves the equation (6) in one dimension using the cross sections generated by CEPXS. To compare the results produced by the two codes, we use equivalent angular discretization, Gauss-Legendre for ONELD, and Gauss-Legendre-Chebyshev(GLC) for our code. The GLC quadrature consists of a Gauss-Legendre quadrature for the polar angle and a Chebyshev quadrature for the azimuthal angle. The n -points Chebyshev quadrature uses n points equally spaced between 0 and 2π . When the solution is independent of the azimuthal angle, the GLC quadrature is equivalent to the one dimensional Gauss-Legendre quadrature. The results of ONELD gives only the average dose on a cell while the results of our code gives the dose at a given point. To compare the dose at any given point, we have interpolated the values given by ONELD.

4.1 Aluminium

The setup of this problem, is the same as that of the previous one except now the medium is composed of aluminium. In the following table, we show the dose computed every centimeter using a different scattering order :

Table I: Dose in $\frac{MeV}{g}$ for different scattering orders

Position	ONELD	order = 13	order = 11	order = 9	order = 7	order = 5
0	0.015003	0.0146404	0.0146402	0.0141156	0.0166718	0.0087276
1	0.169908	0.1697907	0.1697890	0.1698012	0.1695422	0.1728969
2	0.275425	0.2752749	0.2752729	0.2753298	0.2742052	0.2775113
3	0.316307	0.3161310	0.3161307	0.3165279	0.3145572	0.3199176
4	0.312283	0.3120572	0.3120566	0.3125514	0.3104412	0.3153226
5	0.233048	0.2087631	0.2087634	0.2094064	0.2061794	0.2154810

The agreement between ONELD and our code using the full order is excellent. The differences on the edges of the domain are larger, due to the fact that the dose varies quickly near the border. Because of this, the interpolation used to find the value at a given point by ONELD is not very accurate.

We see that if we discard the results on the edges of the domain, the results obtained by using a P_5 order for the scattering are very close to the ones using the full order in the scattering cross-section expansion. The reason is that the high order flux moments are very small. Below,

we show several flux moments for different groups. The abscissa is the distance in centimeters and the ordinate is the value of the flux in $\frac{\text{particles}}{\text{cm}^2 \text{s}}$.

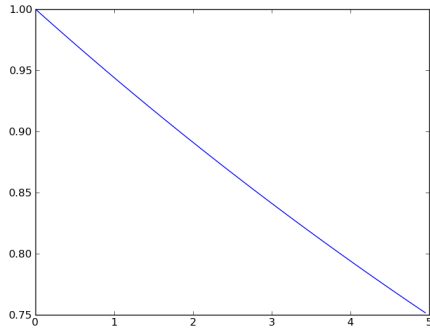


Figure 1: Scalar flux in the first photon group

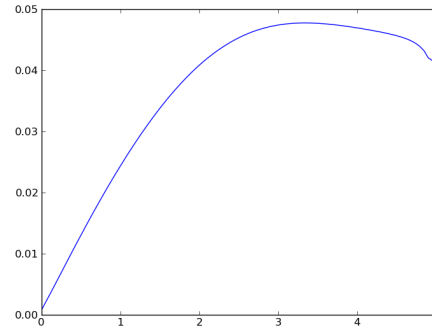


Figure 2: Scalar flux in the last electron group

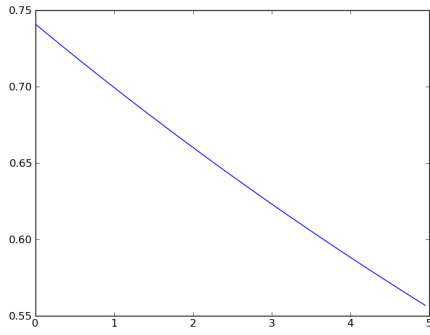


Figure 3: Moment P_5^0 of the flux in the first photon group

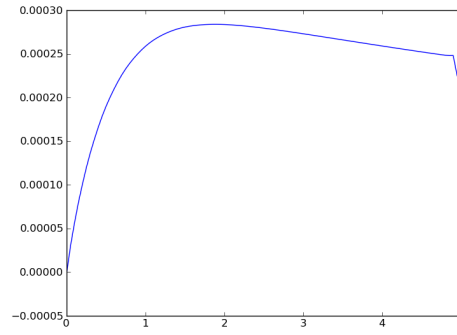


Figure 4: Moment P_5^0 of the flux in the last electron group

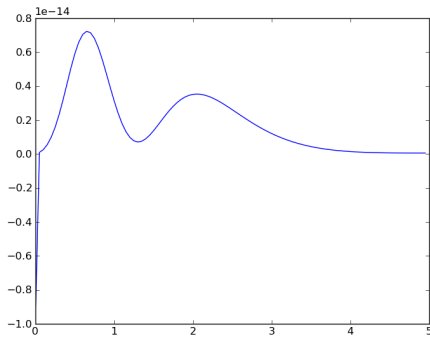


Figure 5: Moment P_{11}^0 of the flux in the first photon group

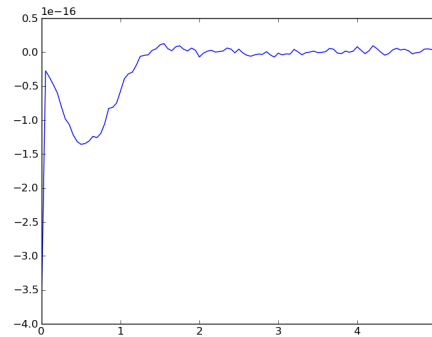


Figure 6: Moment P_5^0 of the flux in the last electron group

4.2 Gold

The setup of this problem is the same as for the previous simulations but the medium considered here is gold. In the next table, we provide the dose computed every centimeter using a different scattering order :

Table II: Dose in $\frac{MeV}{g}$ for different scattering orders

Position	ONELD	order = 11	order = 9	order = 7	order = 5
0	0.11675	0.097168	0.097155	0.097073	0.097326
1	0.41799	0.420905	0.420871	0.420988	0.421102
2	0.16284	0.164953	0.164946	0.165017	0.164605
3	0.06407	0.065297	0.065300	0.065292	0.065214
4	0.02566	0.026303	0.026304	0.026295	0.026318
5	0.00847	0.006082	0.006083	0.006075	0.006112

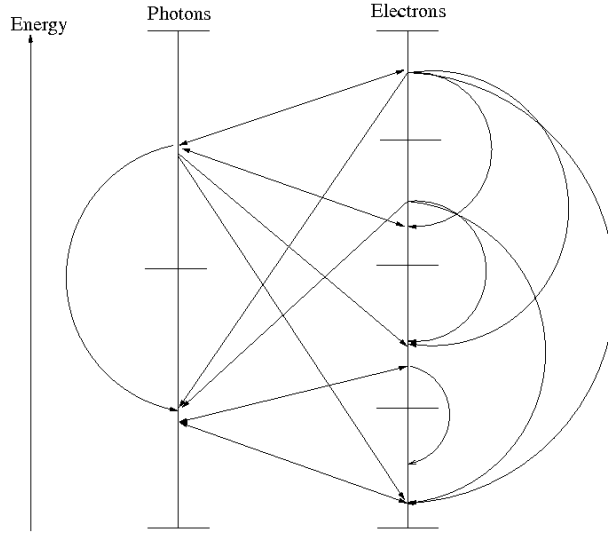
We can see that there is no need to use the full order to solve the problem. The differences between the order 5 and order 11 are small. We do not have the results for the order 13 yet but we do not expect to see the results to be very different from the order 11. The difference between the order 11 and ONELD is about 2% in the middle of the domain. The difference is larger on the boundary of the domain due to the interpolation of the ONELD results.

5. Reordering

Another method to decrease memory needed to solve the transport of photons-electrons deals with reordering the energy groups to simplify the scattering cross-section matrix. When CEPXS generates the cross sections, it first writes all the cross sections for one particle type and then, the cross sections for the other particle type into the scattering matrix. The energy range is the same for the two particles. The cross section matrix looks like :

$$\Sigma = \begin{pmatrix} PP & EP \\ PE & EE \end{pmatrix} \quad (13)$$

where PP and EE are lower triangular matrices which represent the scattering for each particle type. The two matrices are lower triangular because only down scattering is allowed; the cut-off energy used in radiotherapy approximations forbids the thermalization of particles. Matrix EP represents the creation of photons by electrons through bremsstrahlung production and fluorescence production. Matrix PE represents the creation of electrons by photons through photo-electric effect, Compton scattering, pair electron production and Auger production following photoionization. Now it is important to notice that because of energy conservation, a particle can only create a particle which has a energy equal or lower than its own. For example, if there are two photons groups and four electrons groups, the transfers between the groups will look like :

**Figure 7: Transfer between the different groups**

The pattern of the scattering matrix is as follows :

$$\Sigma = \left(\begin{array}{cc|cccc} x & 0 & x & x & 0 & 0 \\ x & x & x & x & x & x \\ \hline x & 0 & x & 0 & 0 & 0 \\ x & 0 & x & x & 0 & 0 \\ x & x & x & x & x & 0 \\ x & x & x & x & x & x \end{array} \right) \quad (14)$$

We can see that there is no upscattering to the first group of photons, the first and the second group of electrons coming from the second group of photons, and the third or the fourth group of electrons (see figure 7). Thus, if we reorder the groups using for the first group set : photon group 1, electron group 1, electron group 2 and for the second group set : photon group 2, electron group 3, electron group 4. The pattern of the scattering matrix looks like :

$$\Sigma = \left(\begin{array}{ccc|ccc} x & x & x & 0 & 0 & 0 \\ x & x & 0 & 0 & 0 & 0 \\ x & x & x & 0 & 0 & 0 \\ \hline x & x & x & x & x & x \\ x & x & x & x & x & 0 \\ x & x & x & x & x & x \end{array} \right) \quad (15)$$

Now, we see that the matrix is block lower triangular and we can solve the transport problem by solving two problems with only three groups each. We can solve the first three groups without solving the last three groups since there is no upscattering coming from these. Then, we can solve the last three groups, with the first three groups hidden in the source term. Thus, we can solve a problem with six groups using the same memory that we would use for only three groups. To know how many groups we need to gather from each particle in each group set, we can use a simple rule. First, we define the number of groups of photons as n_p , the number of

groups electrons as n_e and the greatest common divisor between these two numbers as gcd . The number of groups of photons to put in a group set is $\frac{n_p}{gcd}$ and the number of groups of electrons to put in a group set is $\frac{n_e}{gcd}$. Instead of solving one problem of n groups, we can solve gcd problems of $\frac{n}{gcd}$ groups.

Reordering the groups is also advantageous to decrease the number of iterations of source iteration or GMRES needed to solve a problem. These two methods are used to solve the linear system created by the discretized transport equation of (6). Below, we compare the number of iterations needed to solve a problem very similar to the one of the previous section with and without reordering. The domain is made of aluminium, we use a S_{12} angular discretization and P_5 expansion for the scattering cross section. We use linear discontinuous finite elements for the spatial discretization, there are 1800 cells and we have 15 groups of photon and 25 groups of electron. We obtain the following result :

Table III: Comparison of the number of iterations with and without group reordering

With reordering	Without reordering
7594	7968

The saving is about 4.7% fewer iterations.

At this time, we cannot compare the number of iterations when we reorder the groups and then split the problem in subproblems with our code. When we split the problem in subproblems with our code, we solve all the groups at the same time. All the groups of a subproblem are solved simultaneously and therefore, we cannot take full advantage of the decrease of number of iterations. When we reorder the groups, we mix photon and electron groups and since the photons converge faster, we need to do some extra iterations that are useless for the photons but needed for the electrons. If we split the problems without reordering, the photon groups are solved together in a few iterations. Because there is no extra iterations to solve the photon groups, we need fewer iterations if we do not reorder the groups. We plan to modify our code to take advantage of the reordering.

6. Conclusions

In this paper, we have shown that it is not necessary to keep the full order of the scattering cross sections to obtain an accurate answer while solving photon-electron transport. Truncating the Galerkin quadrature allows us to decrease significantly the memory needs. We also presented a method to advantageously reorder the energy groups in the scattering matrix. The groups can be reordered in such a way that a problem with n_p groups of photons and n_e groups of electrons can be rewritten as gcd problems of $\frac{n_p+n_e}{gcd}$ groups, where gcd is the greatest common divisor between n_p and n_e . The reordering also decreases the number of iterations needed to solve the multigroup transport equation. These two methods combined allow to decrease significantly the memory needed to solve electron transport.

REFERENCES

1. Oleg N. Vassiliev, Todd A. Wareing, John McGhee, Gregory Failla, Mohammad R. Salehpour, and Firas Mourtada. Validation of a new grid-based boltzmann equation solver for dose calculation in radiotherapy with photo beams. *Physics in Medicine and Biology*, 55, 2010.
2. J. Seco, E. Adams, M. Bidmead, M. Partridge, and F. Verhaegen. Head-and-neck imrt treatments assessed with a monte-carlo dose calculation engine. *Physics in Medicine and Biology*, 50, 2005.
3. Thomas Krieger and Otto A Sauer. Monte-carlo- versus pencil-beam-/collapsed-cone-dose calculation in a heterogeneous multi-layer phantom. *Physics in Medicine and Biology*, 50, 2005.
4. J. E. Morel. A hybrid collocation-galerkin-sn method for solving the boltzmann transport equation. *Nuclear Science and Engineering*, 101, 1989.
5. Cepxs/oneld 1.0 manual user. *RSICC Computer Code Collection*.
6. J.E. Morel and D.P. Sloan. A hybrid multigroup/continuous-energy monte-carlo method for solving the boltzmann-fokker-planck equation. *Nuclear Science and Engineering*, 124, 1996.
7. J.E. Morel. Fokker-planck calculations using standard discrete ordinates transport codes. *Nuclear Science and Engineering*, 79, 1981.
8. Kent A. Gifford, John L. Horton Jr., Todd A. Wareing, and Gregory Failla Firas Mourtada. Comparison of a finite-element multigroup discrete-ordinates codes with monte-carlo for radiotherapy calculations. *Physics in Medicine and Biology*, 51, 2006.